

Broadband dielectric spectroscopy of nanocomposites based on PVDF and expanded graphite

This content has been downloaded from IOPscience. Please scroll down to see the full text.

2014 IOP Conf. Ser.: Mater. Sci. Eng. 64 012003

(<http://iopscience.iop.org/1757-899X/64/1/012003>)

View [the table of contents for this issue](#), or go to the [journal homepage](#) for more

Download details:

IP Address: 161.111.22.69

This content was downloaded on 22/06/2015 at 10:10

Please note that [terms and conditions apply](#).

BROADBAND DIELECTRIC SPECTROSCOPY OF NANOCOMPOSITES BASED ON PVDF AND EXPANDED GRAPHITE

A Linares¹, JC Canalda¹, A Sanz¹, A Szymczyk², Z Roslaniec² and TA Ezquerra¹

¹Instituto de Estructura de la Materia (IEM-CSIC), C/ Serrano 121, 28006 Madrid, Spain

²West Pomeranian University of Technology, Institute of Material Science and Engineering, Piastow Av. 19, PL-70310 Szczecin, Poland

E-mail: alinares@iem.cfmac.csic.es

Abstract. Nanocomposites based on poly (vinylidene fluoride) (PVDF) and expanded graphite (EG) were prepared by non-solvent precipitation from solution with different EG concentrations. Films were obtained by compression molding and their structural and dielectric properties studied. From Wide Angle X-ray Scattering (WAXS) experiments, it can be assessed that for all EG concentrations the α -crystalline phase of PVDF is the predominant crystalline form. However, for composites with high nanoadditive content, higher than 3 wt.%, the β -crystalline phase is also detected. Dielectric spectroscopy results showed that the nanocomposites present both high dielectric constant and electrical conductivity at low percolation threshold.

1. Introduction

Nanoadditives based on carbon are receiving increasing attention because of the unique properties of their nanocomposites in comparison with those of traditional composites [1]. Recently graphene and expanded graphite (EG) [2] have attracted considerable interest due to its extraordinary characteristics. Poly(vinylidene fluoride) (PVDF) is a technologically important polymer because of its high dielectric constant, mechanical strength, and resistance to solvents, acids, and bases [3]. Moreover, due to its piezo- and pyroelectric activity this polymer has found use in electromechanical and thermoelectrical transducers. PVDF having a repeat unit of $[-\text{CH}_2 - \text{CF}_2 -]$ is known to exhibit at least four crystalline phases, known as α , β , γ and δ [4]. All these phases differ structurally and the conditions under which a specific conformation can be obtained depend strongly on the processing and thermal or mechanical treatments that the polymer undergoes. It is known that improved electrical performances



such as high dielectric constant, piezoelectricity and pyroelectricity are obtained if PVDF presents β -phase and, to a lesser extent, γ -phase. In this work, we prepare nanocomposites based on PVDF and expanded graphite with different compositions. Providing a comprehensive study of this type of composites can be of great importance because of their broad applications in electrochemical systems such as sensors, electromagnetic interference absorbers and high-charge storage capacitors among others.

2. Experimental

Commercial PVDF powder (Aldrich, Spain), with $M_w \sim 534.000$ g/mol, was used as polymer matrix. The nanoadditive was expanded graphite (SGL Carbon SE, Germany), which, as shown in Fig. 1, forms big stacks of densely packed EG particles, producing worm-like aggregates with an average thickness between 450 and 560 nm and graphene platelets size ranged from 16 μm to 46 μm (99%) [2].

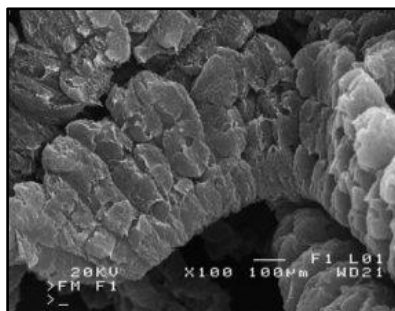


Fig.1. Scanning electron micrograph (SEM) of expanded graphite

N,N-dimethylacetamide (Sigma-Aldrich) was used as solvent and milli-Q quality deionized water as non-solvent. In short, PVDF was dissolved in DMA and different amounts (0.5, 1, 1.5, 1.75, 2, 3 and 4 wt.%) of expanded graphite were also dispersed in DMA. Then, the dispersion of nanoadditive/DMA was added to the PVDF/DMA solution and subsequently the mixture was precipitated into ice distilled water. Then, films of about 1 mm thick were obtained by compression molding. Wide Angle X-ray Scattering (WAXS) measurements were performed by means of a Seifert XRD 3000 h/h diffractometer using Ni-filtered $\text{Cu K}\alpha$ radiation ($\lambda = 0.154$ nm) at a scanning speed of 0.02 $^\circ/\text{s}$. For dielectric experiments, a sandwich geometry was used and circular gold electrodes were deposited onto the surfaces of the film sample. Measurements were performed, at room temperature, over a frequency window of 10^{-2} – 10^7 Hz, using a Novocontrol spectrometer integrating an ALPHA dielectric interface.

3. Results and discussion

3.1. Wide Angle X-ray Scattering (WAXS) results

Fig. 2 shows representative diffraction patterns corresponding to the homopolymer, expanded graphite and some of their nanocomposites. As shown, the diffractogram of PVDF exhibits the characteristic Bragg maxima associated to the (100), (020), (110) and (021) reflections of α -crystalline phase [4]. The pattern corresponding to EG shows the diffraction peak associated to the (002) reflection of the graphitic layer structure.

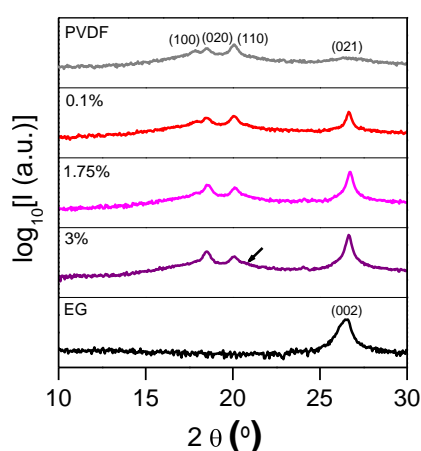


Fig.2. Diffraction patterns of expanded graphite (EG) and of the PVDF/EG nanocomposites for different EG content as labeled

Nanocomposites exhibit mostly the characteristic diffraction maxima corresponding to the PVDF α -crystal phase, being the (021) reflection overlapped by the (002) of the nanoadditive. However, as indicated in Fig. 2 by an arrow, at high nanoadditive content, a shoulder at $2\theta = 20.7^\circ$, which is associated to the (200)/(110) reflections of the β -crystal phase, is also observed. Moreover, it is noteworthy that the (100) reflection decreases and an interchange between the relative intensities associated to (020) and (110) reflections can be observed. This phenomenon has been associated to the nucleation effect of additives in polymer crystallization [5].

3.2. Broadband electrical conductivity

Fig. 3 shows the electrical conductivity as a function of frequency. At low nanoadditive content, $\sigma(F)$ follows a linear dependence with frequency with a slope close to 1, similar to that followed by the insulating PVDF matrix. However, for higher concentrations, $\sigma(F)$ adopts a characteristic behavior which can be formally depicted by the so called universal dynamic response [6] described by a law of the type:

$$\sigma(F) = \sigma_{dc} + \sigma_{ac} = \sigma_{dc} + A F^S \quad (1)$$

where σ_{dc} is the frequency independent direct current conductivity and $0 < S < 1$.

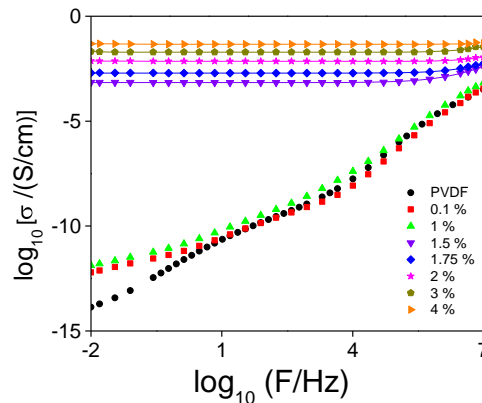


Fig. 3. Broadband electrical conductivity of PVDF/EG nanocomposites for different EG content as labeled

This law introduces a critical frequency, F_c , above which $\sigma(F) = \sigma_{ac} \propto F^S$. The continuous lines in Fig. 3 correspond to fits of eq. 1 to the experimental data. From these fits σ_{dc} values can be extracted. The value of the conductivity at the lowest measured frequency (10^{-2} Hz) for the insulating samples has been considered as σ_{dc} for comparative purpose.

3.2.1 Direct current electrical conductivity

Fig. 4 represents σ_{dc} data as a function of filler concentration. As shown, a characteristic percolating behavior is observed. For low nanoadditive content, the conductivity corresponds to an insulating material. With increasing filler content, at a critical concentration, ϕ_c , the conductivity starts a sudden increase and, according to percolation theory, a continuous network of physically connected particles appears and the insulator–conductor transition occurs. The *dc* conductivity above the critical concentration can be analyzed in terms of the percolation theory [7] by means of:

$$\sigma_{dc} \propto (\phi - \phi_c)^t \quad (2)$$

where t is a critical exponent. Although the critical concentration, ϕ_c , depends on the lattice in which particles are accommodated, t depends primarily on the dimensionality of the percolating system and not on the details of the geometric structures or the interactions [7]. Theoretical calculations [8] propose values of t between 1.6 and 2 for three-dimensional systems. The dashed line in Fig. 4 shows the fittings of eq. 2 to experimental data with t value around 1.4 and $\phi_c \sim 1.31$ wt.%. Below ϕ_c , electrical conductivities higher than that of the

insulating matrix are expected provided that a non-physically connected particles conduction mechanism is present.

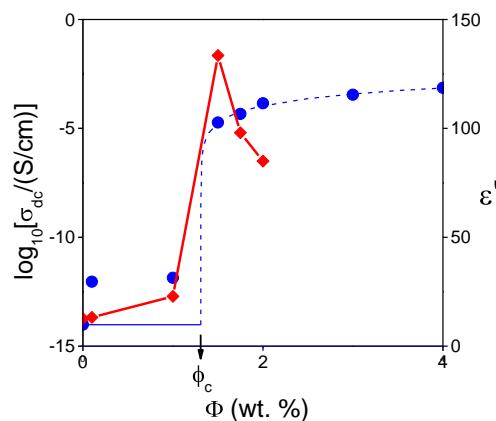


Fig.4. DC electrical conductivity (●) and dielectric constant (◆), at 1000 Hz, for PVDF/EG nanocomposites as a function of the weight concentration of EG

3.2.2 Alternating electrical conductivity

As far as the *ac* conductivity is concerned, Fig. 3 shows that for frequencies above F_c , the frequency dependent conductivity component is observed and the conductivity increases approximately as described by the power law: $\sigma_{ac}(F) \propto F^S$. For these nanocomposites, the *S*-exponent, which is calculated as the slope of the high frequency region in Fig. 3, starts from $S = 1$ (corresponding to insulating specimens) and decreases with increasing nanoadditive concentration until $S \approx 0.8$. Based on the works of Bergman and Imry [9] and Straley [10], the so-called inter-cluster polarization model has been proposed to describe the frequency dependence of conductivity of percolating systems near percolation threshold, ϕ_c . According to this model a value for *S*-exponent ≈ 0.72 can be expected, which is very close to our results. This fact suggests that in this type of nanoadditives, with low aspect ratio, there are a significant amount of polymer interfaces that can contribute to *ac* conductivity through inter-cluster polarization. Likewise, this type of conduction mechanism could also explain the *dc* conductivity behavior observed at nanoadditive concentration below ϕ_c .

3.3 Dielectric constant

Relating to dielectric constant, Fig. 4 shows ϵ' values, taken at 1000 Hz, as a function of the nanoadditive concentration. As can be seen, ϵ' increases with nanoadditive loading. Moreover, near the percolation threshold ϵ' undergoes a remarkable increase. This effect is compatible with the increment of interfaces as nanoadditive concentration increases. In Fig. 4 a clear

maximum is observed, which indicates the concentration at which the amount of interfaces starts to decrease most likely due to the presence of physically connected clusters. At room temperature and 1000 Hz, PVDF presents a value of $\epsilon' \approx 12$, while for the nanocomposite with 1.5 wt.% of EG the ϵ' value is higher than 130.

4. Conclusions

Nanocomposites films based on PVDF and expanded graphite (EG), with different EG concentrations, have been prepared by non-solvent precipitation from solution, and subsequent compression molding. Then, structural and electrical properties have been studied. WAXS studies showed that α -crystalline phase of PVDF is the predominant crystal form in all composites. However, at high content of nanoadditive, the β -crystal phase is also present. Moreover, with increasing EG the intensity of the peak assigned to the (100) reflection decreases, and an interchange between the relative intensities associated to (020) and (110) reflections can be observed. From dielectric spectroscopy analysis, it was concluded that these nanocomposites present high dielectric constant and electrical conductivity at low percolation threshold ($\phi_c \sim 1.31$ wt. %)

5. References

- [1] Linares A *et al* 2008 *Macromolecules* **41** 7090
- [2] Paszkiewicz S *et al* 2012 *J. Polym. Sci. Part B-Polym. Phys.* **50** 1645
- [3] Kerbow D L and Sperati C A 1999 *Physical Constants of Fluoropolymers, Polymer Handbook 4th ed.* (New York, Wiley)
- [4] Lovinger A J 1982 *Developments in Crystalline Polymers* (London, Applied Science)
- [5] García-Gutiérrez M C *et al* 2008 *Macromolecules* **41** 844
- [6] Kremer F and Schönhals A 2002 *A Broad band Dielectric Spectroscopy* (Berlin, Springer)
- [7] Stauffer D 1985 *Introduction to Percolation Theory* (London, Taylor&Francis)
- [8] Connor M T *et al* 1998 *J. Phys. Rev. B* **57** 2286
- [9] Bergman D J and Imry Y 1977 *Phys. Rev. Lett.* **39** 1222
- [10] Straley J P 1977 *Phys. Rev. B* **15** 5733

Acknowledgements

The authors thank the financial support from the Spanish Ministry of Science and Innovation (MICINN), Grant MAT2012-33517 and from the Polish National Science Centre and the Slovak Academy of Sciences in the frame of ERA-NET project APGRAPHEL.